NSRRC- J05205 (2016)

Journal of Materials Chemistry C

PAPER

View Article Online
View Journal | View Issue

Published on 04 May 2016. Downloaded by National Chiao Tung University on 15/07/2016 04:14:02.

Cite this: J. Mater. Chem. C, 2016, 4, 5231

Highly-integrated, laser manipulable aqueous metal carbonyl vesicles (MCsomes) with aggregation-induced emission (AIE) and aggregation-enhanced IR absorption (AEIRA)†

Nimer Murshid,[a] Ken-ichi Yuyama,[b] San-Lien Wu,[b] Kuan-Yi Wu,[b] Hiroshi Masuhara,[b] Chien-Lung Wang[b] and Xiaosong Wang*[a]

Received 23rd March 2016,
Accepted 3rd May 2016

DOI: 10.1039/c6tc01222a

www.rsc.org/MaterialsC

A highly-integrated, laser manipulable multi-functional metal carbonyl nanovesicle (MCsome) with aggregation-induced emission (AIE) and aggregation-enhanced IR absorption (AEIRA) is created *via* the self-assembly of a bithiophene tethered-Fp acyl derivative (Fp: $CpFe(CO)_2$) (**1**). Although **1** is hydrophobic and non-surface-active, the molecule can self-assemble in water into vesicles without detectable critical aggregation concentration (CAC). The water–carbonyl interaction (WCI) is responsible for the colloidal stability. The bilayer membrane structure with the bithiophene moieties associated within the inner wall and the iron-carbonyl units exposed to water is confirmed by transmission electron microscopy (TEM), atomic force microscopy (AFM), and cyclic voltammetry (CV) experiments. The synchrotron small-angle X-ray scattering (SAXS) experiment suggests that the bithiophene groups are interdigitated within the membrane. The spatial segregation of the AIE-active bithiophene domain from the iron-carbonyl units by the butanoyl spacers prevents the quenching effect of the iron and renders the MCsome photoluminescent. The polarizable iron-carbonyl groups on the surface of the MCsome create an enhanced optical field upon infrared (IR) irradiation, resulting in an enhancement (*ca.* 100-fold) in IR absorption for the carbonyl groups as compared to the same concentration of molecule **1** in THF. When the MCsome interacts with a focused continuous-wave near-IR (NIR) laser beam, a strong gradient (trapping) force is generated allowing the laser trapping of the MCsome without using additives. A sharp contrast in the refractive index (RI) of **1** (RI = 1.71) with water (RI = 1.33) accounts for this laser manipulability that is difficult to be achieved for nanosized liposomes (RI = 1.46). As illustrated, the MCsome of **1** represents a novel group of vesicular colloids, which is amenable to functional materials complementary to extensively studied liposomes and polymersomes.

Introduction

Supramolecular chemistry[1] aims to establish a knowledge system for nanomaterial innovation *via* the investigation of the self-assembly behaviour of various building blocks and their aggregation-induced functions.[2] Based on the newly emerged metal carbonyl (MC) supramolecular chemistry,[3,4] highly-integrated, laser manipulable MC vesicles (MCsomes) with aggregation-induced emission (AIE) and aggregation-enhanced IR absorption (AEIRA) have been created in a designed fashion.

MC complexes are potentially useful for a range of biomedical applications, including CO delivery due to their anti-inflammatory effects,[5] antitumor activity due to their selective cytotoxicity,[6] cell imaging[7] and bioassay[8] by taking advantage of the IR absorption of the CO groups within a biologically transparent window at wavelengths between 1800 and 2200 cm^{-1}.[9] Their water solubility,[10] cell uptake ratio[11] and IR absorption intensity[12] can be enhanced using colloidal chemistry.[13] For example, a water-soluble CO-delivery system with a high cell uptake ratio has been developed *via* the incorporation of ruthenium carbonyl complexes into a block copolymer micelle,[11] and IR signals of the CO groups can be enhanced *via* surface enhanced IR absorption (SEIRA) by integrating MC compounds on the surface of plasmonic or dielectric nanoparticles.[12]

[a] *Department of Chemistry and Waterloo Institute for Nanotechnology, University of Waterloo, 200 University Avenue West, Waterloo, Ontario, N2L 3G1, Canada. E-mail: xiaosong.wang@uwaterloo.ca*
[b] *Department of Applied Chemistry and Institute of Molecular Science, National Chiao Tung University, Hsinchu 30010, Taiwan*

† Electronic supplementary information (ESI) available: Laser trapping theory, quantum yield measurement, synthetic schemes and detailed characterization of 1, additional AFM images, DLS, SLS, UV-vis and RI analyses. See DOI: 10.1039/c6tc01222a

Published on 04 May 2016. Downloaded by National Chiao Tung University on 15/07/2016 04:14:02.

Aqueous MC colloids with light emission are highly desirable to promote a further study of the materials, because photoluminescent techniques have been well established and widely used for biomedical investigations.[14] However, photoluminescent MC colloids, unlike their organic counterparts,[15] cannot be readily achieved using fluorochromes, because most transition metal elements are fluorescence (FL) quenchers.[16] To address this challenge, it is desirable to develop assembling techniques enabling the spatial segregation of fluorochromes and MC complexes within the colloids.

We have initiated a study of MC supramolecular chemistry and discovered that hydrophobic Fp acyl derivatives (Fp: $CpFe(CO)_2$), including small and macromolecules,[3] are able to self-assemble in water resulting in MCsomes. These colloids show no critical aggregation concentration (CAC) and exhibit high structural integration upon dilution. Water–carbonyl interaction (WCI) is responsible for the colloidal stability.[3] For example, FpC6 ($CpFe(PPh_3)(CO)CO(CH_2)_5CH_3$)[3a] is able to assemble into a liposome-like bilayer structure with the alkyl chains aggregated within the membrane and the iron complexes associated on the surface. On the basis of this emerged knowledge, we intend to design MC colloids with FL readout. A spatial separation of the conjugated group from the MC complex can be expected, if the MCsome is assembled from an Fp building block tethered to a conjugated system *via* an alkyl spacer. This separation will eliminate the quenching effect of the Fe elements.[16] The crux of the design concerns the selection of an appropriate conjugated system. It is well known that the association of conjugated systems may result in aggregation-caused quenching (ACQ) *via* π–π interactions.[17] In addition, strong π–π interactions, particularly those arising from planar polycyclic aromatic hydrocarbon,[18] may also disturb the balance of the forces responsible for the formation of MCsomes. With this concern in mind, bithiophene, a non-planar small conjugated system,[19] may minimize the possibility of π–π interaction. Although bithiophene groups are non-FL due to the intramolecular rotations of the thiophene units, AIE resulted from the restriction of intramolecular rotations (RIR) can be expected when the conjugated groups are aggregated in an ordered assembled nanostructure.[18]

In addition to the targeted FL readout, the highly polarized MC groups with possibly large refractive indices (RIs) may endow the MCsome with novel properties that liposomes and polymersomes cannot achieve,[20] such as aggregation-enhanced IR absorption (AEIRA)[3] and optical manipulability. Optical trapping of nanosized vesicles, *e.g.* liposome, using focused near-IR laser beams is challenging.[21] The contribution of the difference in RIs between the lipid membrane (RI ~ 1.46) and water (RI = 1.33) to the gradient (trapping) force is negligible, because the membrane is too thin.[21,22] Encapsulation of high refractive index additives, *e.g.* sucrose,[21a] glucose and NaCl,[22] to enhance the trapping forces has been reported to address this challenge. The MCsome with polarizable MC groups may offer a high contrast in RI between the membrane and water, which is expected to enhance the trapping force substantially.[23] Manipulation of the MCsome without additives will, therefore, be possible. This expected advance will open up new opportunities for studying the stability of the colloids,[24] cell membrane-related biological events[25] and their functions in drug delivery.[26]

Herein, we report our innovation in the creation of functional MCsomes *via* the synthesis and self-assembly of a bithiophene tethered Fp derivative (**1**). The building block is hydrophobic, non-surface-active, but is capable of assembly in water *via* WCI, resulting in a MCsome. The MCsome with a bilayer interdigitated membrane, as confirmed by a number of techniques, is highly integrated upon dilution. As designed, the MCsome possesses a number of functions, including AIE, AEIRA of the CO groups and the capability of laser trapping without using additives. These novel functions and unusual solution behaviour of the MCsomes[3] represent a novel group of vesicles and open up a new research topic of MC supramolecular materials.[5–12]

Results and discussion

Synthesis and solution behaviour of 1

The building block (**1**), as designed, contains an iron carbonyl and a bithiophene unit connected *via* a butanoyl spacer. Fig. 1a illustrates the synthetic approach for the targeted molecule. Detailed synthetic scheme and characterization are described in the ESI.† The aqueous solution of **1** is prepared through a fast injection of water into a THF solution of **1** followed by N_2 bubbling to remove THF. The resulting solution is cloudy with a bluish tint (Fig. 1b), suggesting the formation of colloidal particles. DLS analysis of the solution reveals that the hydrodynamic radius (R_h) for the prepared colloids (154 μM) is *ca.* 85 nm with a narrow polydispersity (PDI = 0.05).

It is necessary to use THF as a co-solvent for the preparation because **1** is neither soluble nor dispersible in water. This hydrophobicity of the building block is supported by the ^1H NMR spectrum of **1** in D_2O. As shown in Fig. 2a, no protons corresponding to **1** are detectable; the signal at 4.7 ppm is due to the residual H_2O. As a result of this hydrophobicity, the solution behaviour of **1** is unique. Fig. 2b illustrates that there is no obvious change in surface tension of the solutions as the concentration of **1** decreases, so **1** is non-surface-active. DLS count rates of the solutions as a function of concentration show a linear relationship (Fig. 2c), and no CAC can be deduced from the figure. While we dilute an aqueous solution of **1**, there is no change in both R_h and PDI (Fig. 2d). For all the measurements,

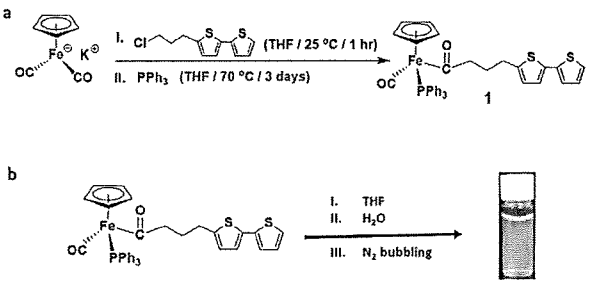

Fig. 1 (a) Schematic illustration for the synthesis of **1**. (b) Aqueous solution of **1** (154 μM) prepared using THF as a co-solvent.

 This journal is © The Royal Society of Chemistry 2016

Published on 04 May 2016. Downloaded by National Chiao Tung University on 15/07/2016 04:14:02.

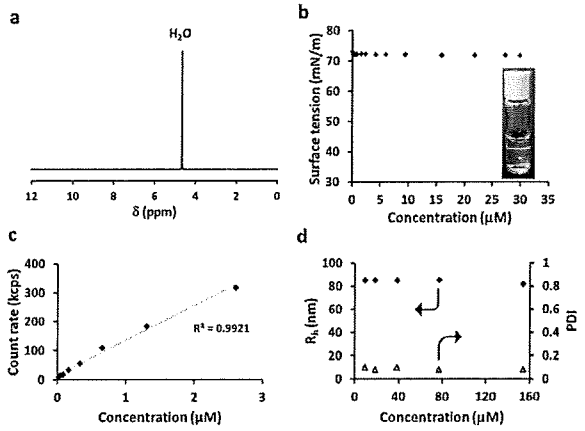

Fig. 2 (a) ^{1}H NMR spectrum of the colloids of **1** in D_2O (154 μM). (b) Surface tensions of **1** in water with varied concentrations. (c) DLS count rates of the aqueous colloids of **1** as a function of concentration. (d) Hydrodynamic radii (R_h) and polydispersity indices (PDI) for the aqueous colloids of **1** with varied concentrations prepared by successive dilution with water. The inset photograph in (b) shows the aqueous solution of **1** (30 μM).

the R_h remains to be 85 nm with PDIs lower than 0.10 (Fig. 2d). These analyses suggest that **1** cannot be classified as a conventional amphiphile.[27] The Fp acyl derivatives therefore represent a new group of building blocks for aqueous colloids without CAC.[3] This feature renders the MC building blocks highly desirable for some applications, such as drug delivery, where traditional surfactant micelles encounter difficulties due to the disassociation of the micelles at concentrations lower than their CACs.[24,28]

We have reported that WCI is a motif responsible for the aqueous self-assembly of Fp acyl derivatives that contains acyl and terminal CO groups.[3] Water can readily hydrate the highly polarized acyl CO group, which balances the hydrophobic force for the formation of the colloids in THF/water upon aggregation at the critical water content.[3a] The aggregation generates a local electric field, which further polarizes the CO groups. Consequently, the strength of the WCI is enhanced, resulting in an aggregation-induced hydration (AIH) of the terminal CO group and an aggregation-enhanced hydration (AEH) of the acyl CO group.[3a] This knowledge was deduced from the IR analysis of the CO groups as a function of water content. A similar analysis has been performed for **1** and the results are illustrated in Fig. 3. As shown in Fig. 3, a red shift in wavenumber for the IR absorption ($\Delta\nu$) of the acyl CO group is observed as soon as water is added to the THF solution of **1**, whereas the IR absorption for the terminal CO group starts to shift only when the water content reaches 60 vol%. This comparison indicates that the acyl CO is more prone to hydration as expected.[3a] When the water content reaches 80 vol%, the $\Delta\nu$ values (7.0 cm^{-1}) for the terminal and acyl CO groups are the same (Fig. 3), suggesting that both CO groups have the same level of hydration. This high $\Delta\nu$ values (7.0 cm^{-1}) for the terminal CO in **1**, compare to that for non-thiophene Fp analogue FpC6 (4.0 cm^{-1}),[3] could be responsible for the increase in the colloidal stability (Fig. S4, ESI†). These results

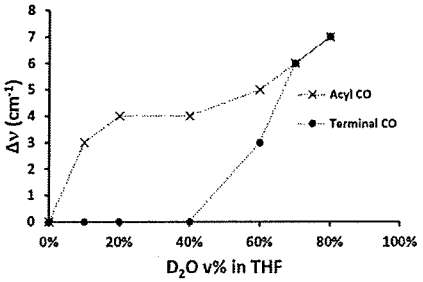

Fig. 3 The red shifts ($\Delta\nu$) in wavenumber for the IR absorption of the terminal and acyl carbonyl groups from **1** in THF/D_2O solutions as a function of D_2O content.

suggest that the WCI plays a crucial role in the colloidal stability (Fig. S4, ESI†). These findings can serve as a model system to understand the biological functions of WCI.[29]

Nanostructure of the MCsome

The radius of gyration (R_g) for colloid **1** is 83.6 nm as measured using the static light scattering (SLS) technique (Fig. S5, ESI†); while R_h, for the same sample obtained from DLS, is 87.1 nm. The shape factor (R_g/R_h) is, therefore, deduced to be *ca.* 0.96, supporting that molecule **1** self-assembles into vesicles in water.[3,30] The conventional transmission electron microscopy (TEM) technique has been attempted to image the colloid and a representative TEM image is shown in Fig. 4a, from which lamellae are observed. The observed morphology may result from the breakage of vesicles. An atomic force microscope (AFM) was subsequently used to verify it. The AFM specimen was prepared *via* drying a few drops of the solution on a mica substrate.

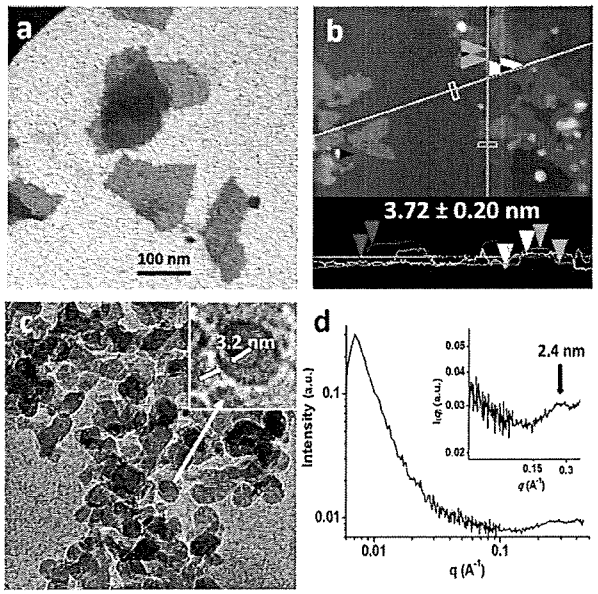

Fig. 4 (a) TEM image, (b) AFM image with vertical section analysis and (c) cryo-TEM images for the colloids of **1**. (d) SAXS profile for the aqueous colloids of **1** (15.4 μM). Insets in (c) and (d) are the enlargements of the selected areas.

Published on 04 May 2016. Downloaded by National Chiao Tung University on 15/07/2016 04:14:02.

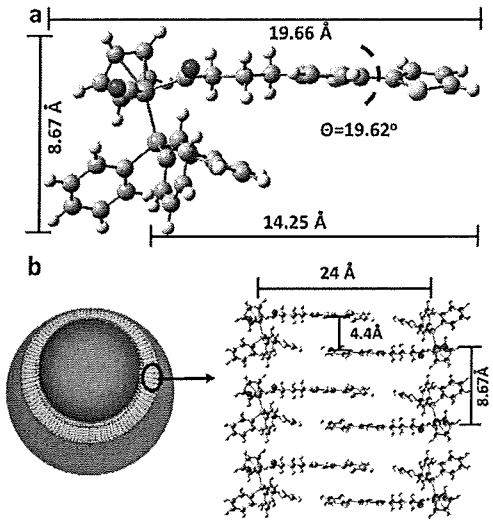

Fig. 5 (a) Gaussian simulation results for molecular geometry of **1**. (b) Proposed interdigitated model for the bilayer membrane structure for the MCsome **1**.

As shown in Fig. 4b, lamellae are observed, which is consistent with the TEM analysis (Fig. 4a). The section analysis reveals that the lamellae have an average vertical height of 3.72 ± 0.20 nm (Fig. 4b and Fig. S7, ESI†), which represents the membrane thickness of the broken vesicle. Cryo-TEM confirms that the colloid is spherical before drying from water (Fig. 4c). The enlarged image (inset in Fig. 4c) shows a dark periphery with a width of *ca.* 3.2 ± 0.7 nm. On the basis of the microscopy experiments, a bilayer membrane structure can be proposed because the fully extended length for **1** is *ca.* 1.9 nm (Fig. 5a). To confirm the bilayer structure and the wall thickness of the MCsome, small-angle X-ray scattering (SAXS) using synchrotron radiation was performed.[31] As shown in Fig. 4d, although the signal intensity is low due to the low concentration of the sample (15.4 μM), a weak hump at q = 0.26 ($Å^{-1}$) is observed, corresponding to a domain spacing of 2.4 nm between the iron elements on the two sides of the membrane. The distance from the iron centre to the end of the bithiophene is *ca.* 14.25 Å (Fig. 5a and Fig. S8a, ESI†), so the bilayer with a iron-to-iron distance of 2.4 nm suggests that the thiophene units are interdigitated as illustrated in Fig. 5b.

The zeta potential (ζ) of the MCsome as measured is −55.5 mV, suggesting that the highly polarized CO ligands are packed on the surface of the vesicle membrane and interacted with water *via* WCIs.[3] CV experiments support this membrane structure with a MC surface. Fig. 6 illustrates the CV curves for the solutions of **1** in DMF/water with varied water contents. In pure DMF solution, **1** is soluble and redox active due to the presence of Fe elements. Its CV curve reveals one oxidation peak at 0.61 V and one reduction peak at 0.51 V (a in Fig. 6). After water is added, two oxidation peaks separated by a redox coupling ($\Delta E_{1/2}$) appears (b and c in Fig. 6), suggesting that iron centers are associated closely with each other[3a,32] and accessible to the electrodes. In pure water, although the MCsome is stable due to the WCI, no oxidation signals are

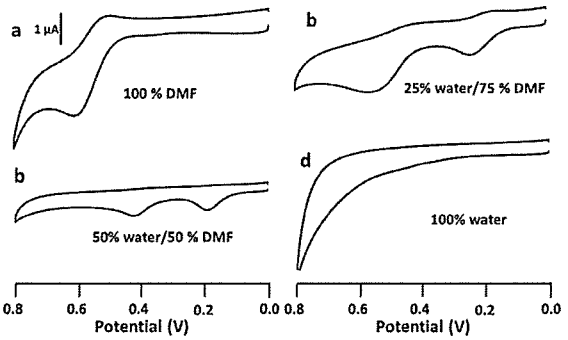

Fig. 6 Cyclic voltammetry (CV) analyses, relative to the Ag electrode, for the solutions of **1** in DMF/water with different water contents.

detectable (d in Fig. 6). This behaviour is similar to that observed for the non-thiophene analogue FpC6[3a] and can be attributed to the hydrophobic nature of **1**.

Aggregation induced emission (AIE) of the MCsome

The association of the bithiophene moieties within the inner walls of the bilayer vesicles restricts the intramolecular rotation of the thiophene units and, therefore, AIE is expected.[33] As shown in Fig. 7a, the MCsome in water emits blue FL when exposed to a UV light, whereas the molecule of **1** in THF does not emit light. The solid sample of **1** dried from the aqueous solution (Fig. 7c) also has no photoluminescence (Fig. 7d). This comparison indicates that the bilayer assembly of **1** is crucial for the observed AIE (Fig. 5b). The butanoyl spacer separates the conjugated system from the iron elements, which prevents the quenching of the emission.[16]

The solution emitted the strongest FL emission when excited by the light with a wavelength of 360 nm (λ_{ex} = 360 nm). The intensity for the FL emission is decreased when λ_{ex} is lower or higher than 360 nm (Fig. S9, ESI†), but there is no obvious shift in the maximum emission wavelength (454 ± 2 nm) with λ_{ex} = 310–360 nm (Fig. S9a, ESI†). However, higher excition wavelength generates multiple emission peaks (Fig. S9b, ESI†). All the following experiments are excited by λ_{ex} = 350 nm.

FL spectra and photographs of the solutions in THF/water with varied amounts of water are illustrated in Fig. 7b. As shown in Fig. 7b, one may notice that the emission appears even for the solution containing a small amount of water (9 vol%). If there was no aggregation at this low water content (9 vol%), AIE might not be the reason for the emission. We therefore performed DLS experiments for a series of THF/water solutions with varied water contents from 0 to 100 vol%. Fig. 8a displays the light scattering count rates as a function of water content; the corresponding hydrodynamic radii (R_h) and FL emission intensities of the solutions are plotted in Fig. 8b. As depicted in Fig. 8a, a steep enhancement in count rates occurs at a water content of 60 vol%. However, the count rates start to increase and micron-size aggregates are formed (Fig. 8b) when the water content is only 9 vol%. Therefore, the emission at the low water content (9 vol%) can be attributed to the aggregation as well (Fig. 7b). The aggregates gradually shrink from micron-size

 This journal is © The Royal Society of Chemistry 2016

Published on 04 May 2016. Downloaded by National Chiao Tung University on 15/07/2016 04:14:02.

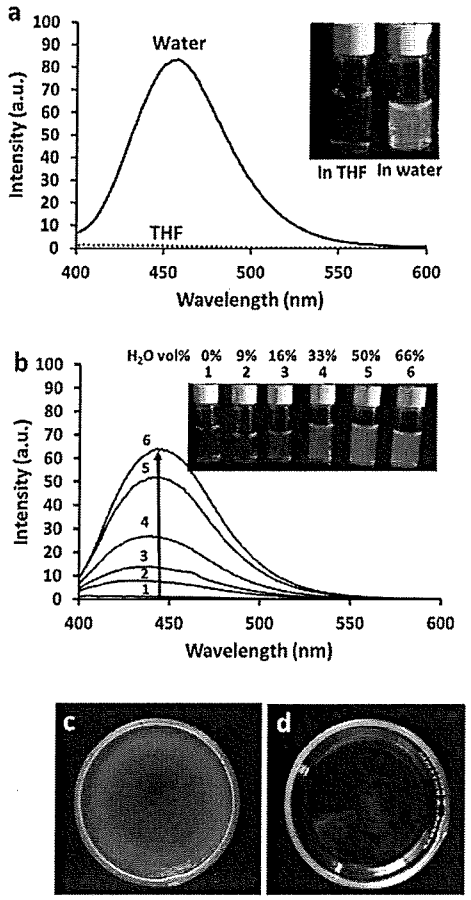

Fig. 7 (a) Fluorescence emission spectra for the solutions of **1** (154 μM) in THF and water. (b) Fluorescence emission spectra for the solutions diluted from **1** in THF (154 μM) by the addition of varied amounts of water. Photographs for the water solution of **1** (c) before and (d) after drying. The photographs, including insets for (a)–(d), are taken when the samples are irradiated with a UV lamp (λ_{ex} = 350 nm).

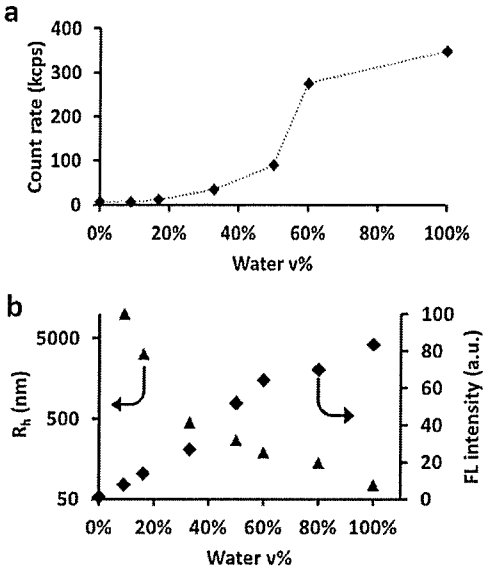

Fig. 8 (a) DLS count rates, (b) R_h and FL fluorescence intensities for THF/water solutions of **1** as a function of water content.

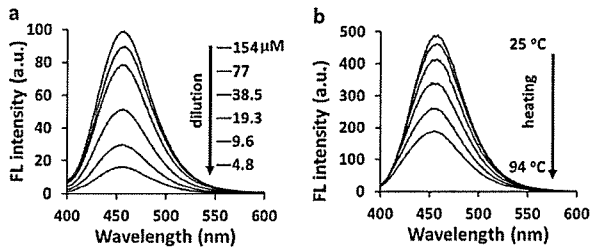

Fig. 9 (a) FL emission spectra for the aqueous MCsome prepared by successive dilution of an aqueous colloid of **1** (154 μM). (b) FL emission spectra of the aqueous colloids of **1** (154 μM) measured at different temperatures (λ_{ex} = 350 nm).

to 450, 190, and 85 nm, as the water content increases to 30, 60 and 100 vol%, respectively (Fig. 8b). The RIR of the bithiophene groups is enhanced following this shrinkage, resulting in an enhancement in FL intensity as shown in Fig. 8b.

Meanwhile, there are no strong π–π interactions between the bithiophene groups because no obvious red shifts in wavelength are observed for both emission and absorption spectra of **1** in THF/water with water contents less than 80% (Fig. 7b and Fig. S10, ESI†). A slight red shift in the maximum absorption wavelength is observed from the UV-vis spectrum when the water content reaches 80 vol%, suggesting that the π–π interaction starts to occur at a higher water content (Fig. S10, ESI†). However, this tendency is competed and suppressed by the steric hindrance of the bulky MC groups (Fig. 5),[18,34] which minimizes the ACQ, and RIR remains a major factor influencing the emission. Besides, the curvature of the vesicular bilayer assembly may also reduce the possibility of a face-to-face packing of the bithiophene units and consequently prevent a strong ACQ effect.[17,35] Therefore, the AIE is obviously observed even in pure water (Fig. 7a). The quantum yield (QY) for the aqueous colloid of **1**, as compared with 1,4-bis(5-phenyloxazol-2-yl) benzene (POPOP) in cyclohexane,[36] is *ca.* 7.27 (see the ESI†).

The MCsome is able to emit light even if the solution is diluted to 4.8 μM (Fig. 9a and Fig. S11, ESI†). These results agree with DLS results (Fig. 2d) and suggest that the MCsome of **1** possesses a highly integrated structure and colloidal stability upon dilution. Furthermore, this AIE is also temperature sensitive. As shown in Fig. 9b, the FL intensity deceases when the solution is heated. After cooling back to 25 °C, the original FL intensity is recovered. DLS analysis indicates that the diameter of the aggregates increases by 20 nm upon heating from 25 °C to 94 °C. Therefore, the reversible AIE can be explained by the variation of RIR resulted from the temperature-stimulated swellability of the MCsome.[37] The uniform and highly integrated MCsomes with temperature-sensitive photoluminescence are therefore potentially useful as drug delivery systems,[38] sensors and bioimaging probes.[39]

Similar to the THF/water solutions, the AIE phenomenon is also observed for the solutions of the MCsomes in dimethyl sulfoxide (DMSO)/water and acetonitrile (CH_3CN)/water (Fig. S12, ESI†).

Published on 04 May 2016. Downloaded by National Chiao Tung University on 15/07/2016 04:14:02.

Meanwhile, by varying the pH of the solution from 3 to 10, there is no obvious change in the emission profile in terms of intensity and emission wavelength (Fig. S13, ESI†), so the MCsomes are potentially useful for biological applications.

AEIRA and laser manipulability of the MCsome

Another unique feature of the MCsome is the highly polarized MC surface that endows the colloid with novel properties. It is well studied that polarized nanoparticles, *via* interaction with incident light, are able to generate a strong local electromagnetic field applicable for SEIRA.[40] Fig. 10 displays the IR absorptions of the terminal CO group for the MCsome solutions in THF/water as a function of water content. As shown in Fig. 10, although the concentration of **1** (154 μM) for all the solutions are the same, the IR absorption for the solution with 60 vol% of water is *ca.* 100 times stronger than those for the systems with lower water contents. This AEIRA is also observed for the MCsome assembled from other MC building blocks,[3] supporting that this feature results from the MC groups. A 100-fold enhancement in IR absorption has also been reported for the anthracene adsorbed on the surface of silicon carbide particles,[41] and is explained due to the phonon resonance effect caused by the dielectric surface,[41] which is analogous to the plasmon resonance of metal substrates, a basis for surface-enhanced Raman scattering (SERS)[42] and SEIRA.[43] It is therefore reasonable to think that the surface of the MCsome with tightly associated polarizable MC groups behaves like dielectric substrates responsible for the observed AEIRA. MCsomes possess a surface with polarized CO groups, which induce a local electric field with a zeta potential of −55.5 mV. Upon irradiation of IR, the local electric field interacts with the electromagnetic field of the illuminated light and becomes stronger than incident light. This stronger electric field enhances the absorption intensity of the CO groups located at the surface of the MCsomes.[3a,40b,41] This enhancement is desirable and potentially useful for bioassay and cell imaging.[12]

The advent of the MCsome offers opportunities to address a challenge in vesicle studies using focused near-infrared (NIR) laser beams. It has been proposed that cell membranes can be studied *via* laser trapping of liposomes as model systems.[44] However, despite several attempts,[22,45] laser manipulation of nanosized liposomes with thin membranes remains to be challenging.[21]

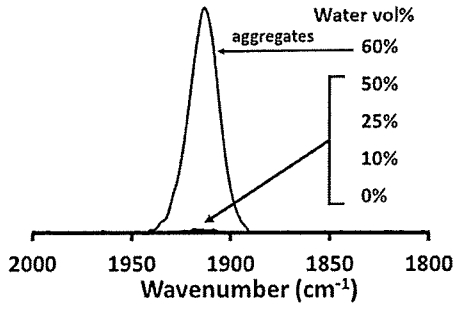

Fig. 10 Partial ATR-FTIR spectra (terminal CO) of **1** in THF/water solutions with varied water contents.

Although the RI of the lipids (1.46) is different from that of water (1.33), the contribution of this marginal difference to the trapping forces is found to be negligible.[23,46] The MCsome assembled from a highly polarizable MC building block may resolve this problem. Although the membrane for the MCsome is only *ca.* 3.7 nm, the RI for the building block (1.71 at λ = 633 nm) (Fig. S14, ESI†) is significantly higher than lipids (1.46) and water (1.33). The high contrast in the RI between the membrane and water may result in a trapping force strong enough to trap the MCsome without using additives.[23,47] Therefore, we performed the laser trapping experiments (Fig. 11a). As shown in Fig. 11b, the aggregation of the vesicles appears at the focal point after the solution of MCsome (77 μM) is irradiated with a focused continuous-wave near-IR (NIR) laser beam for 1 second. More MCsomes are attracted to the focal point by prolonging the irradiation time. The images taken at 3 and 6 seconds indicate that the aggregates become larger with improved contrast (Fig. 11b). After irradiation for 6 seconds, the size of the aggregate remains constant, suggesting that the focal volume is fully occupied by the MCsomes and the laser trapping reaches the equilibrium state. The solution (77 μM) was subsequently diluted 4, 8, 16, and 32 times for further experiments. The laser trapping reached equilibrium states after the solutions were irradiated for *ca.* 20, 35, 60, and 90 seconds, respectively (Fig. 11c). As shown in Fig. 11c, the MCsomes, due to its

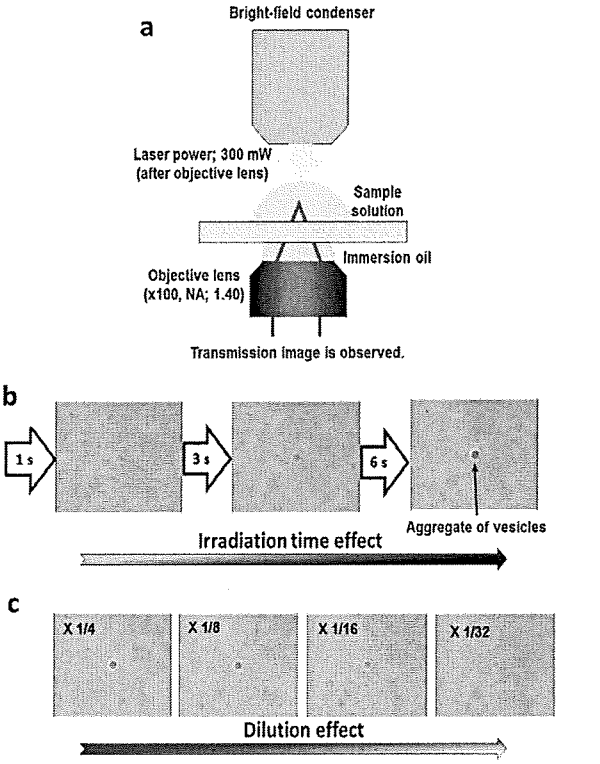

Fig. 11 (a) Experimental set-up for laser-trapping experiments. (b) The charge-coupled device (CCD) transmission images of the trapped MCsome recorded at 1, 3 and 6 seconds. (c) CCD transmission images, taken at the equilibrium states, for samples diluted from the MCsome solution (77 μM) by 4, 8, 16 and 32 fold. The image size is 48 μm in width and 36 μm in height.

This journal is © The Royal Society of Chemistry 2016

Published on 04 May 2016. Downloaded by National Chiao Tung University on 15/07/2016 04:14:02.

high integration upon dilution, are trapped even for the sample with the concentration of 2.3 μM. It is also found that the gathered MCsomes can be moved arbitrarily following the beam and released upon turning off the trapping laser, which verifies the success of the trapping experiments. Thus, the MCsome shows good laser manipulability without additives, which is difficult to be achieved for liposomes.[21]

Conclusions

Bithiophene-tethered Fp acyl derivative (**1**) is hydrophobic and non-surface-active, but is able to self-assemble in water into a metal carbonyl vesicle (MCsome). The MCsome is colloidally stabilized by WCI and highly integrated upon dilution. The bilayer membrane structure of the MCsome is confirmed by TEM, AFM, CV and SAXS experiments. The bithiophene component is aggregated within the inner wall of the interdigitated membrane and spatially separated from the MC groups associated on the surface of the MCsome, resulting in AIE. The aggregation of the polarizable MC component with a high refractive index endows the particle with novel functions, such as AEIRA and laser manipulability without using additives. The solution behaviour and the properties of the MCsomes are unique and desirable as a new group of vesicular materials, complementary to the extensively studied liposomes[48] and polymersomes[20] for potential applications,[5–12] including nanoreactors,[49] sensors[50] and drug delivery systems.[51]

Experimental section

Materials and instrumentation

Potassium metal (99.5%, rods in mineral oil) and sodium metal (99.9%, cubes in mineral oil), a cyclopentadienyl iron(II) dicarbonyl dimer (99%), 2,2′-bithiphene (97%), benzophenone (99%) and 1-bromo-3-chloropropane (>98.0%) were purchased from Sigma-Aldrich and used as received. Triphenylphosphine (98%) was purchased from Tokyo Chemical Industry (TCI) and used as received. Tetrahydrofuran (THF) was distilled over sodium/benzophenone before use. All other solvents were obtained from local commercial providers and used as received.

Dynamic light scattering (DLS) analyses were performed using a Zetasizer Nano Series (Nano-S90, Malvern Instruments) with a laser wavelength of 633 nm at a fixed angle of 90°. For THF/water solutions with varied water contents, the samples are prepared by the successive addition of water to a THF solution of **1** (154 μM). Multi-angle SLS measurements were carried out using a Brookhaven Laser Light Scattering System equipped with a BI-200 SM goniometer. A vertically polarized helium–neon diode laser with a wavelength of 636 nm was used as the light source. Measurements were taken at scattering angles (θ) between 50° and 130° with 10° intervals. Toluene was used as the reference for the Rayleigh ratio. Zeta potential (ζ) measurement was performed at 25 °C on a Malvern Zetasizer nano ZS instrument using disposable folded capillary cells. The surface tension of pure water and the aqueous colloids of **1** with different concentrations was measured at 24 °C using a tensiometer Data Physics DCAT 21 system. Cyclic voltammetry (CV) experiments for solutions of **1** (154 μM) in water/DMF were performed at room temperature using a DY2000 Multi-Channel Potentiostat (Digi-Ivy Inc.) workstation with a scan rate of 50 mV s^{-1} and silver wire as a reference electrode. A water solution of KCl (2 mg mL^{-1}) and a DMF solution of tetrabutylammonium perchlorate (TBAP) (2 mg mL^{-1}) were prepared. **1** was then dissolved in the DMF solution and the water solution was subsequently added to prepare the solutions of **1** in water/DMF.

^{1}H and ^{31}P nuclear magnetic resonance (NMR) spectra were recorded on a Bruker-300 (300 MHz) spectrometer at room temperature. ^{1}H NMR chemical shifts were reported relative to a residual $CDCl_3$ signal and ^{31}P NMR resonances were referenced to an external standard sample of 85% H_3PO_4 (δ = 0.0). Attenuated total reflection-Fourier transform infrared (ATR-FTIR) spectra for the solid sample of **1** were recorded on a Bruker Tensor 27 spectrophotometer with a resolution of 1 cm^{-1}. Pellets were prepared by grinding and compressing of **1** (2% by weight) in anhydrous KBr using Nujol mulls. The ATR-FTIR spectra of **1** in THF/water solutions were recorded on the same instrument using a germanium crystal Pike MIRacleTM ATR Attachment using Pike Technologies. A drop of the solution was placed on the germanium crystal. IR absorption of the solutions of **1** in THF was measured first. Afterward, water was successively added to the THF solution and IR spectra were recorded at different water contents.

Conventional transmission electron microscopy (TEM) images were recorded on a low voltage (5 kV) LVEM5 electron microscope (Delong Instruments). TEM samples were prepared by dropping the solution onto a carbon-coated copper grid (Cu-300CN, Pacific rid Tech) and the grid was then left to dry at ambient temperature. Cryo-TEM images were obtained using a high voltage (200 kV) field emission FEI Tecnai G2 F20 Cryo-TEM microscope. The cryo-TEM sample was prepared by applying a 5.0 μL aqueous solution of **1** (154 μM) onto a glow discharged copper grid with holy carbon film (Quantifoil Multi A) and thinned by blotting with a filter paper. The grid was then quickly plunged into a liquid ethane bath and transferred under liquid nitrogen to a Gatan 914 cryo-holder and viewed at −179 °C. Atomic force microscopy (AFM) experiments were conducted on a Nanoscope MultiModeTM AFM microscope using a Conical AFM tip with a spring constant of 40 N m^{-1}, a resonance frequency of 300 KHz and tip radius of 8 nm. The sample was prepared by transferring 2 drops of the aqueous colloids of **1** on a freshly sliced mica substrate.

Steady-state fluorescence emission spectra were recorded using a Cary Eclipse Fluorescence Spectrophotometer. A conventional quartz cell with a light path of 1 cm was used for the solution samples. The solutions were excited at a λ_{ex} of 350 nm. UV-vis absorption spectra were recorded on a Varian (Carey 100 Bio) UV-vis spectrophotometer using a quartz cuvette with a path length of 1 cm. The refractive index was obtained using a J. A. Woollam Co. VASE® ellipsometer. Data were required at angles of incidence of 55°, 60°, 65°, 70°, and 75° in a spectral

Published on 04 May 2016. Downloaded by National Chiao Tung University on 15/07/2016 04:14:02.

range from 1700 to 400 nm. The measurement was performed for a thin film prepared by spin-coating of 5 wt% solution of **1** in toluene on a silicon wafer (Fig. S14, ESI†).

The SAXS data were acquired at Beamline 23A1 in the National Synchrotron Radiation Research Center (NSRRC), Taiwan. The energy of the X-ray source and the sample-to-detector distance were 15 keV and 2977.4 mm. The aqueous solution of **1** (15.4 μM) was introduced into a sample cell consisting of two Kapton windows. To collect the scattering signals, a two-dimensional MarCCD detector with a resolution of 512 × 512 pixels was used. The SAXS profile was corrected for the empty cell beam scattering, sample transmission, and detector sensitivity. The domain spacing (d) was calculated by $d = 2\pi/q_m$ (q_m: the position of the primary scattering peak). The q range of the small-angle X-ray scattering (SAXS) measurement is between 0.008 and 0.40 $Å^{-1}$ (d = 78.5–1.6 nm). Since the R_h of the colloids of **1** (87.1 nm) is above the detection upper limit, the SAXS data were used to estimate the wall thickness of the MCsome. Quantum-chemical calculations were performed using the Gaussian09 suite employing the DFT calculations (B3LYP/6-311G). Geometry optimizations were performed using tight SCF and convergence criteria.

For laser trapping experiments, a small amount of the sample solution was put onto a glass substrate (Matsunami, micro cover glass, thickness; 0.12–0.17 mm) placed on the stage of an inverted microscope (Olympus, IX71). A 1064 nm continuous-wave near-infrared laser beam (Spectra Physics, J20I-BL-106C, λ = 1064 nm) was used as the trapping light source and was focused to a position a few tens of micrometers above the glass through an objective lens (100 magnification, NA = 1.4, oil immersion). The laser power was fixed to 300 mW after the objective lens by adjusting a half-wave plate placed in front of a polarizing beam splitter. The trapping behavior was observed using a charge-coupled device (CCD) camera (WATEC, WAT-231S2) under halogen-lamp illumination. Laser trapping theory is described in the ESI.†

Synthesis of 5-[3-chloropropyl]-2,2′-bithiophene (1)

Molecule 5-[3-chloropropyl]-2,2′-bithiophene (**1**) was prepared as follows. *n*-Butyl lithium (*n*-BuLi) (5.41 mmol) was added dropwise to a solution of 2,2′-bithiophene (1 g, 6.01 mmol) in THF (100 mL) at −78 °C under an atmosphere of dry nitrogen. After stirring for 0.5 h at −78 °C, 1-bromo-3-chloropropane (595 μL, 6.01 mmol) was slowly added. The reaction mixture was then warmed gradually to room temperature and stirred overnight. The solvent was removed by rotary evaporation and the residue was subsequently purified using column chromatography on silica gel with hexane as the eluent (yield 0.684 g, 47%). ^{1}H NMR ($CDCl_3$, 25 °C, 300 MHz) δ (ppm): 2.14 (Q, 2H; middle $-CH_2-$), 2.98 (t, 2H; BTh–CH_2-), 3.59 (t, 2H; $-CH_2-Cl$), 6.73 (d, 1H; BTh), 7.00 (m, 2H; BTh), 7.11 (d, 1H; BTh), 7.17 (d, 1H; BTh). The detailed synthesis scheme is illustrated in Scheme S1 and the ^{1}H NMR spectrum of **1** is shown in Fig. S1 in the ESI.†

The purified molecule **1** (0.684 g, 2.82 mmol) was then added to a solution of the Fp anion (0.67 g, 3.10 mmol) in THF (50 mL) at 0 °C under vigorous stirring. The mixture was stirred at room temperature (23 °C) for 1 hour. Triphenylphosphine (0.81 g, 3.10 mmol) was then added to the mixture and subsequently refluxed at 70 °C for 72 hours. Afterward, the solution was cooled to room temperature and THF was removed under vacuum. The resulting gold-brownish solid was chromatographed using a silica column with hexane/DCM (2/1 v/v) as the eluent. The solvents were removed using rotary evaporation resulting in a brownish foam-like product (yield 1.45 g, 79%). ^{1}H NMR ($CDCl_3$, 25 °C, 300 MHz) δ (ppm): 1.35 (m, 2H; middle $-CH_2-$ from the spacer), 2.41 (t, 2H; BTh–CH_2-), 2.67 (m, 1H; $-CO-CH_2-$), 2.90 (m, 1H; $-CO-CH_2-$), 4.41 (s, 5H; Cp ring), 6.57 (d, 1H; BTh), 6.9–7.0 (m, 2H; BTh), 7.07 (d, 1H; BTh), 7.14 (d, 1H; BTh) 7.37 (s, 9H; *o*- and *p*-Ph), 7.49 (t, 6H; *m*-Ph). ^{31}P NMR ($CDCl_3$, 25 °C, 300 MHz) δ (ppm): 77.4. FT-IR (KBr pellet, 25 °C): 1600 cm^{-1} (acyl C=O), 1905 cm^{-1} (terminal C≡O). The ^{1}H, ^{31}P NMR and FT-IR spectra of **1** are shown in Fig. S2 and S3 in the ESI.†

Self-assembly of 1

The aqueous colloids of **1** (154 μM) were prepared by fast addition of 10.0 mL of distilled deionized water to a 1.0 mL THF solution of **1** (1.0 mg mL^{-1}, 1.54 mM) under stirring. THF was then removed through nitrogen bubbling for 90 minutes. The same experiment was performed in D_2O and examined using ^{1}H NMR, which suggested that THF is completely removed.

Acknowledgements

Nature Science and Engineering Research Council of Canada (NSERC RGPIN-402137-2011), the University of Waterloo and the Waterloo Institute for Nanotechnology (WIN) are acknowledged for financial support. Aklilu Worku is acknowledged for AFM imaging. Nathan Nelson-Fitzpatrick is acknowledged for performing ellipsometry experiments. H. M. (MOST 103-2113-M-009-003) and K. Y. (MOST 103-2113-M-009-022-MY2) acknowledge the MOE-ATU Project (National Chiao Tung University) of the Ministry of Science and Technology (MOST) and the National Science Council of Taiwan for financial support.

Notes and references

1 (*a*) J.-M. Lehn, *Angew. Chem., Int. Ed. Engl.*, 1990, **29**, 1304–1319; (*b*) T. Aida, E. W. Meijer and S. I. Stupp, *Science*, 2012, **335**, 813–817; (*c*) T. F. A. De Greef, M. M. J. Smulders, M. Wolffs, A. P. H. J. Schenning, R. P. Sijbesma and E. W. Meijer, *Chem. Rev.*, 2009, **109**, 5687–5754.

2 (*a*) E. Elacqua, D. S. Lye and M. Weck, *Acc. Chem. Res.*, 2014, **47**, 2405–2416; (*b*) T. R. Cook, Y.-R. Zheng and P. J. Stang, *Chem. Rev.*, 2013, **113**, 734–777; (*c*) F. Würthner, C. R. Saha-Möller, B. Fimmel, S. Ogi, P. Leowanawat and D. Schmidt, *Chem. Rev.*, 2016, **116**, 962–1052; (*d*) A. Harada, Y. Takashima and M. Nakahata, *Acc. Chem. Res.*, 2014, **47**, 2128–2140; (*e*) C. Rest, R. Kandanelli and G. Fernàndez, *Chem. Soc. Rev.*, 2015, **44**, 2543–2572; (*f*) H. Qiu, Z. M. Hudson, M. A. Winnik and I. Manners, *Science*, 2015, **347**,

 This journal is © The Royal Society of Chemistry 2016

Published on 04 May 2016. Downloaded by National Chiao Tung University on 15/07/2016 04:14:02.

1329–1332; (*g*) F. H. Schacher, P. A. Rupar and I. Manners, *Angew. Chem., Int. Ed.*, 2012, **51**, 7898–7921; (*h*) S. I. Stupp and L. C. Palmer, *Chem. Mater.*, 2014, **26**, 507–518; (*i*) Y. Wang, H. Xu and X. Zhang, *Adv. Mater.*, 2009, **21**, 2849–2864; (*j*) D. G. Kurth, *Sci. Technol. Adv. Mater.*, 2008, **9**, 014103; (*k*) G. M. Whitesides and B. Grzybowski, *Science*, 2002, **295**, 2418–2421; (*l*) J. Kang, D. Miyajima, T. Mori, Y. Inoue, Y. Itoh and T. Aida, *Science*, 2015, **347**, 646–651; (*m*) Z. Yu, F. Tantakitti, T. Yu, L. C. Palmer, G. C. Schatz and S. I. Stupp, *Science*, 2016, **351**, 497–502; (*n*) T. Haino, *Polym. J.*, 2013, **45**, 363–383.

3 (*a*) N. Murshid and X. Wang, *Chem. – Eur. J.*, 2015, **21**, 19223–19230; (*b*) K. Cao, N. Murshid, L. Li, A. Lopez, K. C. Tam and X. Wang, *Macromolecules*, 2015, **48**, 7968–7977.

4 N. Lanigan, A. Assoud and X. Wang, *ACS Macro Lett.*, 2014, **3**, 1281–1285.

5 (*a*) K. Fujita, Y. Tanaka, T. Sho, S. Ozeki, S. Abe, T. Hikage, T. Kuchimaru, S. Kizaka-Kondoh and T. Ueno, *J. Am. Chem. Soc.*, 2014, **136**, 16902–16908; (*b*) H. Tabe, K. Fujita, S. Abe, M. Tsujimoto, T. Kuchimaru, S. Kizaka-Kondoh, M. Takano, S. Kitagawa and T. Ueno, *Inorg. Chem.*, 2015, **54**, 215–220.

6 (*a*) I. Ott, B. Kircher, C. P. Bagowski, D. H. W. Vlecken, E. B. Ott, J. Will, K. Bensdorf, W. S. Sheldrick and R. Gust, *Angew. Chem.*, 2009, **121**, 1180–1184 (*Angew. Chem., Int. Ed.*, 2009, **48**, 1160–1163); (*b*) D. Schlawe, A. Majdalani, J. Velcicky, E. Hessler, T. Wieder, A. Prokop and H. G. Schmalz, *Angew. Chem.*, 2004, **116**, 1763–1766 (*Angew. Chem., Int. Ed.*, 2004, **43**, 1731–1734).

7 C. Policar, J. B. Waern, M.-A. Plamont, S. Clède, C. Mayet, R. Prazeres, J.-M. Ortega, A. Vessières and A. Dazzi, *Angew. Chem., Int. Ed.*, 2011, **50**, 860–864.

8 N. Fischer-Durand, M. Salmain, B. Rudolf, L. Dai, L. Jugé, V. Guérineaud, O. Laprévote, A. Vessières and G. Jaouen, *Anal. Biochem.*, 2010, **407**, 211–219.

9 (*a*) K. Meister, J. Niesel, U. Schatzschneider, N. Metzler-Nolte, D. A. Schmidt and M. Havenith, *Angew. Chem., Int. Ed.*, 2010, **49**, 3310–3312; (*b*) S. Clède and C. Policar, *Chem. – Eur. J.*, 2015, **21**, 942–958.

10 E. Parera, F. Comelles, R. Barnadasz and J. Suades, *Chem. Commun.*, 2011, **47**, 4460–4462.

11 U. Hasegawa, A. J. van der Vlies, E. Simeoni, C. Wandrey and J. A. Hubbell, *J. Am. Chem. Soc.*, 2010, **132**, 18273–18280.

12 R. F. Aroca, D. J. Ross and C. Domingo, *Appl. Spectrosc.*, 2004, **58**, 324A–338A.

13 (*a*) W.-Y. Wong, Q. Dong, S.-H. Cheung, P.-L. Lau, N.-Y. Zhu, Y. H. Lo and H. Li, *J. Cluster Sci.*, 2015, **26**, 461–471; (*b*) J. Zukerman-Schpector, I. Haiduc and E. R. T. Tiekink, *Chem. Commun.*, 2011, **47**, 12682–12684.

14 A. J. Amoroso, M. P. Coogan, J. E. Dunne, V. Fernndez-Moreira, J. B. Hess, A. J. Hayes, D. Lloyd, C. Millet, S. J. A. Pope and C. Williams, *Chem. Commun.*, 2007, 3066–3068.

15 (*a*) A. Shao, Y. Xie, S. Zhu, Z. Guo, S. Zhu, J. Guo, P. Shi, T. D. James, H. Tian and W.-H. Zhu, *Angew. Chem., Int. Ed.*, 2015, **54**, 7275–7280; (*b*) Z. Guo, A. Shao and W.-H. Zhu, *J. Mater. Chem. C*, 2016, **4**, 2640–2646; (*c*) X. Zhang, S. Rehm, M. M. Safont-Sempere and F. Würthner, *Nat. Chem.*, 2009, **1**, 623–629; (*d*) A. Das and S. Ghosh, *Macromolecules*, 2013, **46**, 3939–3949; (*e*) S.-L. Deng, T.-L. Chen, W.-L. Chien and J.-L. Hong, *J. Mater. Chem. C*, 2014, **2**, 651–659; (*f*) E. Ravindran, S. J. Ananthakrishnan, E. Varathan, V. Subramanianabc and N. Somanathan, *J. Mater. Chem. C*, 2015, **3**, 4359–4371.

16 (*a*) L. Prodi, F. Bolletta, M. Montalti and N. Zaccheroni, *Coord. Chem. Rev.*, 2000, **205**, 59–83; (*b*) A. W. Varnes, R. B. Dodson and E. L. Wehry, *J. Am. Chem. Soc.*, 1972, **94**, 946–950.

17 (*a*) Y. Hong, J. W. Y. Lama and B. Z. Tang, *Chem. Commun.*, 2009, 4332–4353; (*b*) G. Chen, W. Li, T. Zhou, Q. Peng, D. Zhai, H. Li, W. Z. Yuan, Y. Zhang and B. Z. Tang, *Adv. Mater.*, 2015, **27**, 4496–4501.

18 Y. Hong, J. W. Y. Lamab and B. Z. Tang, *Chem. Soc. Rev.*, 2011, **40**, 5361–5388.

19 (*a*) A. M. Fedor, D. G. Allis and T. M. Korter, *Vib. Spectrosc.*, 2009, **49**, 124–132; (*b*) J. M. Speck, D. Schaarschmidt and H. Lang, *Organometallics*, 2012, **31**, 1975–1982; (*c*) J. D. Einkauf, L. Mathivathanan and D. T. de Lill, *J. Mol. Struct.*, 2016, **1104**, 33–39.

20 (*a*) P. Tanner, P. Baumann, R. Enea, O. Onaca, C. Palivan and W. Meier, *Acc. Chem. Res.*, 2011, **44**, 1039–1049; (*b*) M. Antonietti and S. Förster, *Adv. Mater.*, 2003, **15**, 1323–1333; (*c*) M. Marguet, C. Bonduelle and S. Lecommandoux, *Chem. Soc. Rev.*, 2013, **42**, 512–529; (*d*) D. E. Discher and A. Eisenberg, *Science*, 2002, **297**, 967–973.

21 (*a*) P. M. Bendix and L. B. Oddershede, *Nano Lett.*, 2011, **11**, 5431–5437; (*b*) D. P. Cherney, J. C. Conboy and J. M. Harris, *Anal. Chem.*, 2003, **75**, 6621–6628; (*c*) S. Park, S. Q. Choi, C. Song, M. W. Kim and M. C. Choi, *Soft Matter*, 2014, **10**, 8406–8412.

22 M. Ichikawa and K. Yoshikawa, *Appl. Phys. Lett.*, 2001, **79**, 4598–4600.

23 T. Sugiyama, K.-I. Yuyama and H. Masuhara, *Acc. Chem. Res.*, 2012, **45**, 1946–1954.

24 S. C. Owena, D. P. Y. Chana and M. S. Shoicheta, *Nano Today*, 2012, **7**, 53–65.

25 T.-H. Lee, D. J. Hirst and M.-I. Aguilar, *Biochim. Biophys. Acta*, 2015, **1848**, 1868–1885.

26 (*a*) T. M. Allen and P. R. Cullis, *Adv. Drug Delivery Rev.*, 2013, **65**, 36–48; (*b*) N. Suwanpayak, M. Jalil, C. Teeka, J. Ali and P. Yupapin, *Biomed. Opt. Express*, 2011, **2**, 159–168.

27 A. Domínguez, A. Fernández, N. González, E. Iglesias and L. Montenegro, *J. Chem. Educ.*, 1997, **74**, 1227–1231.

28 (*a*) K. Letchford and H. Burt, *Eur. J. Pharm. Biopharm.*, 2007, **65**, 259–269; (*b*) B. M. Discher, H. Bermudez, D. A. Hammer and D. E. Discher, *J. Phys. Chem. B*, 2002, **106**, 2848–2854; (*c*) F. Li, T. Ketelaar, A. T. M. Marcelis, F. A. M. Leermakers, M. A. C. Stuart and E. J. R. Sudhölter, *Macromolecules*, 2007, **40**, 329–333.

29 (*a*) Q. Nhu, N. Nguyen, M. W. Lodewyk, S. Bezer, M. R. Gagné, M. L. Waters and D. J. Tantillo, *ACS Catal.*, 2015, **5**, 1617–1622; (*b*) R. Wolfenden, *Biochemistry*, 1978, **17**, 201–204.

Published on 04 May 2016. Downloaded by National Chiao Tung University on 15/07/2016 04:14:02.

30 P. Mahato, S. Saha, S. Choudhury and A. Das, *Chem. Commun.*, 2011, **47**, 11074–11076.
31 (*a*) G. Battaglia and A. J. Ryan, *J. Am. Chem. Soc.*, 2005, **127**, 8757–8764; (*b*) J. A. Bouwstra, G. S. Gooris, W. Bras and H. Talsma, *Chem. Phys. Lipids*, 1993, **64**, 83–98.
32 (*a*) D. A. Foucher, C. H. Honeyman, J. M. Nelson, B. Z. Tang and I. Manners, *Angew. Chem., Int. Ed. Engl.*, 1993, **32**, 1709–1711; (*b*) R. Rulkens, A. J. Lough, I. Manners, S. R. Lovelace, C. Grant and W. E. Geiger, *J. Am. Chem. Soc.*, 1996, **118**, 12683–12695; (*c*) V. V. Dement'ev, F. Cervantes-Lee, L. Parkanyi, H. Sharma, K. H. Pannell, M. T. K. Nguyen and A. F. Diaz, *Organometallics*, 1993, **12**, 1983–1987.
33 (*a*) Z. Chang, Y. Jiang, B. He, J. Chen, Z. Yang, P. Lu, H. S. Kwok, Z. Zhao, H. Qiua and B. Z. Tang, *Chem. Commun.*, 2013, **49**, 594–596; (*b*) J. Luo, Z. Xie, J. W. Y. Lam, L. Cheng, H. Chen, C. Qiu, H. S. Kwok, X. Zhan, Y. Liu, D. Zhuc and B. Z. Tang, *Chem. Commun.*, 2001, 1740–1741.
34 (*a*) W. Tang, Y. Xiang and A. Tong, *J. Org. Chem.*, 2009, **74**, 2163–2166; (*b*) S. Y. Ryu, S. Kim, J. Seo, Y.-W. Kim, O.-H. Kwon, D.-J. Jangb and S. Y. Park, *Chem. Commun.*, 2004, 70–71; (*c*) C. J. Bhongale, C.-W. Chang, C.-S. Lee, E. W.-G. Diau and C.-S. Hsu, *J. Phys. Chem. B*, 2005, **109**, 13472–13482.
35 L. Zhao, Y. Lin, T. Liu, H. Li, Y. Xiong, W. Z. Yuan, H. H.-Y. Sung, I. D. Williams, Y. Zhang and B. Z. Tang, *J. Mater. Chem. C*, 2015, **3**, 4903–4909.
36 A. M. Brouwer, *Pure Appl. Chem.*, 2011, **83**, 2213–2228.
37 (*a*) J. Chen, C. C. W. Law, J. W. Lam, Y. Dong, S. M. F. Lo, I. D. Williams, D. Zhu and B. Z. Tang, *Chem. Mater.*, 2003, **15**, 1535–1546; (*b*) V. Mukundam, K. Dhanunjayarao, R. Mamidala and K. Venkatasubbaiah, *J. Mater. Chem. C*, 2016, **4**, 3523–3530.
38 (*a*) Y. Qiu and K. Park, *Adv. Drug Delivery Rev.*, 2012, **64**, 49–60; (*b*) A. Samad, Y. Sultana and M. Aqil, *Curr. Drug Delivery*, 2007, **4**, 297–305.
39 (*a*) S. Ryu, I. Yoo, S. Song, B. Yoon and J.-M. Kim, *J. Am. Chem. Soc.*, 2009, **131**, 3800–3801; (*b*) Y.-R. Kim, S. Jung, H. Ryu, Y.-E. Yoo, S. M. Kim and T.-J. Jeon, *Sensors*, 2012, **12**, 9530–9550.
40 (*a*) X. Chen, C. Ciracì, D. R. Smith and S.-H. Oh, *Nano Lett.*, 2015, **15**, 107–113; (*b*) M. Osawa, *Top. Appl. Phys.*, 2001, **81**, 163–187.
41 M. S. Anderson, *Appl. Phys. Lett.*, 2003, **83**, 2964–2965.
42 N. Cathcarta and V. Kitaev, *Nanoscale*, 2012, **4**, 6981–6989.
43 (*a*) A. Hartstein, J. R. Kirtley and J. C. Tsang, *Phys. Rev. Lett.*, 1980, **45**, 201–204; (*b*) F. Hahn and C. A. Melendres, *Electrochim. Acta*, 2001, **46**, 3525–3534.
44 (*a*) A. Ashkin, J. M. Dziedzic and T. Yamane, *Nature*, 1987, **330**, 769–771; (*b*) J. B. Hutchison, C. A. Rodesney, K. S. Kaushik, H. H. Le, D. A. Hurwitz, Y. Irie and V. D. Gordon, *Langmuir*, 2014, **30**, 4522–4530; (*c*) Y. Pang, H. Song, J. H. Kim, X. Hou and W. Cheng, *Nat. Nanotechnol.*, 2014, **9**, 624–630.
45 N. Kitamura, N. Sekiguchi and H.-B. Kim, *J. Am. Chem. Soc.*, 1998, **120**, 1942–1943.
46 J. Hotta, K. Sasaki and H. Masuhara, *J. Am. Chem. Soc.*, 1996, **118**, 11968–11969.
47 Y. Harada and T. Asakura, *Opt. Commun.*, 1996, **124**, 529–541.
48 (*a*) S. Deshpande, Y. Caspi, A. E. C. Meijering and C. Dekker, *Nat. Commun.*, 2016, 7, 10447; (*b*) B. Q. Spring, R. B. Sears, L. Z. Zheng, Z. Mai, R. Watanabe, M. E. Sherwood, D. A. Schoenfeld, B. W. Pogue, S. P. Pereira, E. Villa and T. Hasan, *Nat. Nanotechnol.*, 2016, **11**, 378–387; (*c*) M. Karlsson, M. Davidson, R. Karlsson, A. Karlsson, J. Bergenholtz, Z. Konkoli, A. Jesorka, T. Lobovkina, J. Hurtig, M. Voinova and O. Orwar, *Annu. Rev. Phys. Chem.*, 2004, **55**, 613–649.
49 (*a*) D. A. Wilson, R. J. M. Nolte and J. C. M. van Hes, *Nat. Chem.*, 2012, **4**, 268–274; (*b*) J. Gaitzsch, D. Appelhans, L. Wang, G. Battaglia and B. Voit, *Angew. Chem., Int. Ed.*, 2012, **51**, 4448–4451; (*c*) K. T. Kim, J. J. L. M. Cornelissen, R. J. M. Nolte and J. C. M. van Hest, *Adv. Mater.*, 2009, **21**, 2787–2791; (*d*) Y. Elani, R. V. Law and O. Ces, *Nat. Commun.*, 2014, **5**, 5305.
50 (*a*) M. Lomora, F. Itel, I. A. Dinu and C. G. Palivan, *Phys. Chem. Chem. Phys.*, 2015, **17**, 15538–15546; (*b*) S. Haas, N. Hain, M. Raoufi, S. Handschuh-Wang, T. Wang, X. Jiang and H. Schönherr, *Biomacromolecules*, 2015, **16**, 832–841.
51 (*a*) S. Egli, M. G. Nussbaumer, V. Balasubramanian, M. Chami, N. Bruns, C. Palivan and W. Meier, *J. Am. Chem. Soc.*, 2011, **133**, 4476–4483; (*b*) H. Lomas, I. Canton, S. MacNeil, J. Du, S. P. Armes, A. J. Ryan, A. L. Lewis and G. Battaglia, *Adv. Mater.*, 2007, **19**, 4238–4243; (*c*) H. Kim, Y. J. Kang, S. Kang and K. T. Kim, *J. Am. Chem. Soc.*, 2012, **134**, 4030–4033; (*d*) X. Wang, J. Hu, G. Liu, J. Tian, H. Wang, M. Gong and S. Liu, *J. Am. Chem. Soc.*, 2015, **137**, 15262–15275; (*e*) C. Zhou, M. Wang, K. Zou, J. Chen, Y. Zhu and J. Du, *ACS Macro Lett.*, 2013, **2**, 1021–1025.

 This journal is © The Royal Society of Chemistry 2016